On the optical thickness in the UV range: Analysis of the ground-based data taken at Belsk, Poland

Janusz Jarosławski, Janusz W. Krzyścin, Sylwester Puchalski, and Piotr Sobolewski
Institute of Geophysics, Polish Academy of Sciences, Warsaw, Poland

Received 7 March 2003; revised 23 June 2003; accepted 14 August 2003; published 5 December 2003.

[1] The longest time series of UV-B and short wavelength of UV-A aerosol optical depth has been constructed for the period 1992–2002 using the direct Sun irradiances obtained during standard calculations of total ozone by the Brewer spectrophotometer at Belsk (51°84N, 20°78E), Poland. The long-term variations appear to be trendless with only small year-to-year variations. The statistical analysis of the 1-day change of aerosol optical depth in the UV range shows that in 30% of cases the scale of the aerosol change is important for the next day UV index forecast. In the analysis of dependence of the aerosol optical depth on wavelength we combine the CIMEL Sun photometer and the Brewer spectrophotometer optical depth data. The Ångström's exponent is calculated for the pairs of wavelengths in the visible, UV-A, and UV-A/UV-B ranges. It is found that Ångström's exponent decreases for the shorter wavelength pair, and it is possible that in the UV-B/UV-A range the exponent is actually negative, yielding an increase of aerosol optical depth with wavelength. The Mie code simulations corroborate the hypothesis of possible negative values for the Ångström's exponent in the UV-B/UV-A range. *INDEX TERMS:* 0305 Atmospheric Composition and Structure: Aerosols and particles (0345, 4801); 0360 Atmospheric Composition and Structure: Transmission and scattering of radiation; 3359 Meteorology and Atmospheric Dynamics: Radiative processes; *KEYWORDS:* atmospheric radiation, aerosols, UV range

Citation: Jarosławski, J., J. W. Krzyścin, S. Puchalski, and P. Sobolewski, On the optical thickness in the UV range: Analysis of the ground-based data taken at Belsk, Poland, *J. Geophys. Res.*, *108*(D23), 4722, doi:10.1029/2003JD003571, 2003.

1. Introduction

[2] In recent years, increased interest has been noted on studies of the aerosol properties in the ultraviolet (UV) range when it was established that the aerosols could significantly affect the intensity of UV radiation at the ground level. The observed ozone depletion at high and midlatitudes triggered attention to the related increase of the UV radiation at the Earth's surface. Many other factors, such as cloud cover and aerosol loading of the atmosphere may also influence the UV radiation interfering with the ozone related changes. The importance of aerosols on the surface UV was recognized by *Liu et al.* [1991]. They estimated that the surface solar irradiance in the 280–316 nm (biologically active solar radiation, UV-B) had decreased over nonurban Northern Hemisphere mid-latitudinal region by about 10% since the industrial revolution owing to increasing aerosols loading of the atmosphere. According to *Zerefos et al.* [1995], about 25% of the total variability of erythemal irradiance during cloudless conditions at Tessaloniki, Greece, could be attributed to the nonozone forcing (changes in the aerosol properties, albedo, and other pollutants). The UV observations by the Brewer spectrophotometer (BS) revealed that the reduction of the erythemaly weighted UV irradiance at the Earth's surface could reach 10–30% for extreme changes in the aerosol optical depth (AOD) [e.g., *Zerefos*, 1997]. *Krzyścin and Puchalski* [1998] found that the mean impact of the aerosol loading changes on the UV fluctuations in the warm part of the year was comparable with that induced by the total ozone changes. Thus it becomes evident that more specific knowledge of aerosol characteristics in the UV range and their effects on the ground-level UV radiation lead to improved accuracy in the UV climatology modeling, proper scaling of the measured UV spectra, and reliable UV Index forecasting [*Krzyścin et al.*, 2001].

[3] The AOD measurements for the UV-B and short UV-A wavelength are rather difficult and require precise calibration procedures. The atmospheric optical depth due to the Rayleigh scattering ($\sim\lambda^{-4}$) and the ozone absorption are large in the UV-B range but the solar radiation is rather weak as compared to the visible wavelengths. Thus calculation of AOD as the residual optical depth that remains after the elimination of the molecular scattering, ozone and SO_2 absorption effects contains substantial uncertainty. Recently the methodology based on the attenuation of the direct solar irradiance measured by BS has been developed to infer the AOD variations in the UV range. Two approaches have been proposed, first one is based on an absolute calibration of the solar irradiance measured by BS [*Bais*, 1997; *Marenco et al.*, 1997; *Meleti and Cappellani*, 2000] and second one uses the Langley method (Langley method is named for S. P. Langley of the Smithsonian Institute and is based on his work of the early 1900s to

0148-0227/03/2003JD003571$09.00

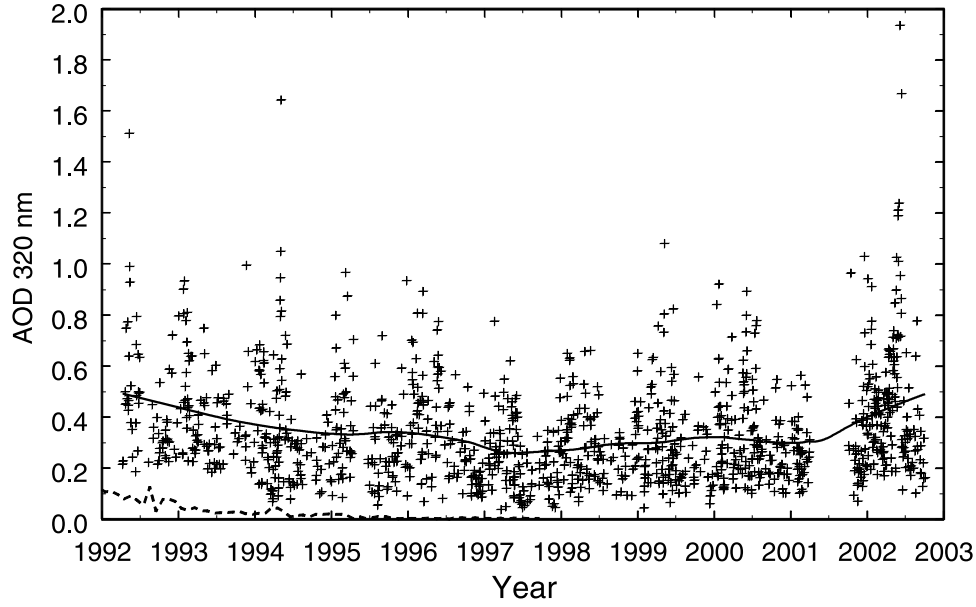

Figure 1. Daily means of aerosol optical depth at 319.8 nm measured at Belsk, Poland, for the period 1992–2002. The solid curve represents the long-term variations of the aerosol optical depth from a smoother (LOWESS) applied to the data points. The dashed curve gives the stratospheric aerosol optical depth variations calculated by SRRB using method of *Stevermer et al.* [2000].

determine the extraterrestrial constant - total amount of incoming solar irradiance at the top of the earth's atmosphere) to obtain an instrumental equivalent of the extraterrestrial constants [*Jarosławski and Krzyścin*, 2000; *Kirchhoff et al.*, 2001; *Marenco et al.*, 2002]. The derived AODs appeared consistent with those measured independently by a multifilter rotating shadow-band radiometer [*Marenco et al.*, 2002] and the CIMEL Sun photometer [*Jarosławski and Krzyścin*, 2000; *Meleti and Cappellani*, 2000].

[4] The purpose of the paper is to analyze AOD data obtained in the period 1992–2002 at Belsk (51°84N, 20°79E), Poland, by the Brewer spectrophotometer Mark II. We focus both on the long-term changes (trend) in the AOD time series and short term (daily and day-to-day) variations of the data. We would like to discuss the aerosol forcing on UV radiation and the impact of day-to-day AOD changes. Since April 2002 observations by a co-located CIMEL Sun photometer have been performed giving continuous AOD monitoring at 340, 380, 440, 500, 660, 870, and 1020 nm. Thus we have an opportunity to analyze the wavelength dependence of the optical thickness emphasizing the difference between the Ångström exponents calculated over the visible and UV wavelength.

2. Measurements and the AOD Retrieval Method

[5] The Brewer spectrophotometer was originally designed to measure the column amount of ozone in the atmosphere [*Brewer*, 1973]. The Belsk's instrument measures solar irradiance in five operational channels, 306.1, 309.8, 313.3, 316.6, and 319.8 nm. The total ozone algorithm uses the combination of measured solar radiances to eliminate the effects of the molecular scattering, scattering and absorption by aerosols, and SO_2 absorption on the UV transmission throughout the atmosphere. The total optical thickness τ is inferred from the UV direct solar irradiance at each wavelength taking into account Beer's law;

$$\tau = \frac{1}{m_a} \ln(I_{o\nu}/I_\nu) \tag{1}$$

where I_ν is the measured radiation intensity at frequency ν, at the Earth's surface, after being attenuated by the medium, $I_{o\nu}$ is the intensity at the top of the atmosphere (the so-called extraterrestrial constant), and m_a is the air mass factor that takes into account the direct beam slant path through the atmosphere. The Langley method allows determining $I_{o\nu}$: the values of the natural logarithm applied to measured UV irradiation intensity are plotted against the pertaining air mass; the slope of the resulting straight line is τ and extrapolated values of I_ν at $m_a = 0$ gives the instrumental representative of the extraterrestrial constant. We estimate extraterrestrial constants (ETC) for each day in the analyzed period as moving means from a set of ETC obtained during the clear-sky days with stable atmospheric conditions over Belsk that had occurred before and after selected day in half year period. In such a way the systematic error connected with ETC estimation and the instrument drift effects on ETC could be minimized.

[6] AOD can then be inferred by subtraction of the contribution of other factors from τ. In the UV range these are the ozone absorption, the Rayleigh scattering, and SO_2 absorption (neglected in this study because of small amount of SO_2 in the atmosphere over Belsk). Therefore

$$\begin{aligned}\tau_{aerosol} &= \tau - \tau_{rayleigh} - \tau_{ozone} \\ &= \tau - p/p_o \tau_{rayleigh,o}(\lambda) - Tot_{O3} k_{O3}(\lambda)\end{aligned} \tag{2}$$

where p is the atmospheric pressure at the measuring site, p_o is standard atmospheric pressure, $\tau_{rayleigh,o}(\lambda)$ is the optical

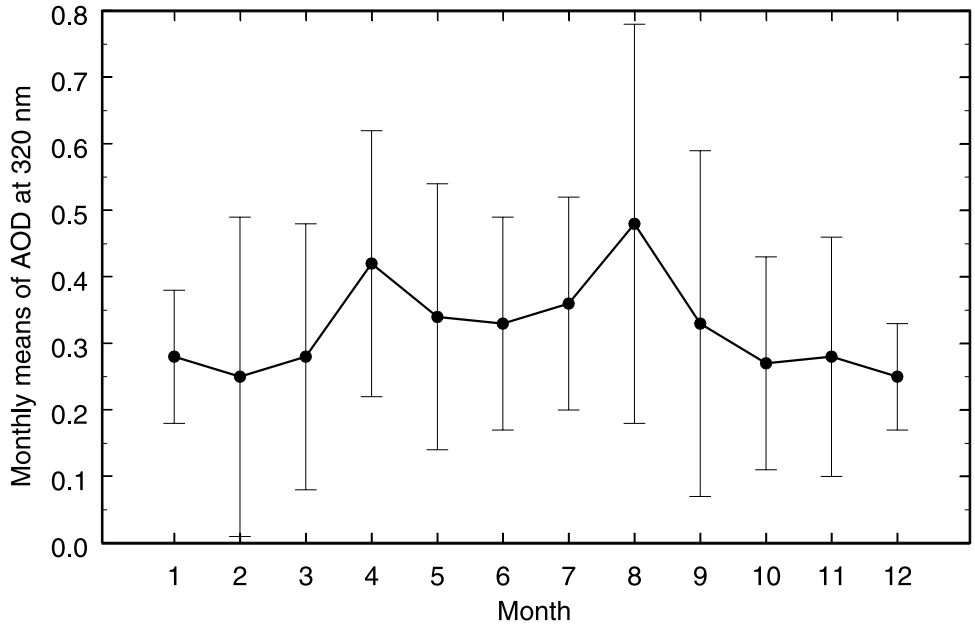

Figure 2. Monthly means of aerosol optical depth at 319.8 nm from the daily measurements by the Brewer spectrophotometer (1992–2002) with ±2σ error bars.

depth due to the Rayleigh scattering calculated at the sea level under standard atmospheric conditions that is approximated by the *Bucholtz* [1995] formula, $\tau_{rayleigh,o}(\lambda) = 0.0065\lambda^{-3.552+0.001356\lambda+115.63/\lambda}$, Tot_{O3} is total ozone, and $k_{O3}(\lambda)$ is the ozone absorption coefficients taken from *Bass and Paur* [1985].

[7] Reliability of described method has been confirmed by the intercomparisons of AOD measurements made by three independently co-located Brewers in Poprad, Slovakia [*Jarosławski and Krzyścin*, 2000] and the co-located CIMEL Sun photometer (see section 3). Results of intercomparisons confirm a correspondence between the CIMEL and BS AOD measurements and good agreement between AODs by various BSs.

[8] Uncertainties associated with AOD measurements were calculated according to the *International Standards Organization (ISO)* [1993] guidelines. For details, see, e.g., *Bernhard and Seckmeyer* [1999]. Two main groups of sources of measurement errors were identified. First group was related with technical parameters of BS, e.g., attenuation filters drifts, temperature coefficients changes, photomultiplier dead time changes, wavelength misalignment, timing errors etc. Second (the most important) group of uncertainties was related to the applied Langley method, e.g., extraterrestrial constants error, total ozone content error, ozone and Rayleigh absorption and scattering coefficients error etc.

[9] The resulting combined uncertainty (with the coverage factor k = 2) for the measurements of AOD in the range 320–310 nm is equal to 0.02, which is similar to the uncertainties of the CIMEL Sun photometer for the measurements of AOD at 340 nm [*Holben et al.*, 2001]. It is worth noting that AODs in the UV-B range are calculated using the temperature corrected Brewer total ozone (accounting for the stratospheric temperature departures from standard temperature −46.3°C assumed by the Brewer retrieval) and values of ozone cross section at actual stratospheric temperatures (see section 4 for more details). Thus the uncertainty comprises mostly the random effects on the AOD retrieval rather than systematic ones.

[10] It looks possible that AOD measurements sometimes may be contaminated by the cloud effects. Special procedure has been applied to exclude cases when the solar disc was obscured by clouds. BS provides almost continuously the atmospheric optical thickness regardless of cloud conditions, so we take into account only those optical thicknesses (and assigned them as AOD) if the pattern of the atmospheric optical thickness is smooth, i.e., the change of optical thickness calculated from neighboring BS observations (time difference between them ∼10 minutes) is less than the AOD uncertainty. Moreover, we analyze the daily course of the global solar radiation by the CM-21 pyranometer and eliminate optical thicknesses collected in periods of abrupt changes of global radiation (global radiation is more sensitive to the cloud effects that the UV radiation).

[11] Method described above has been used for retrieving of AOD for five wavelengths using the archived BS counts (stored during standard procedure of total ozone calculations) for the period January 1992 to December 2002. Since April 2002 AOD measurements at Belsk have been extended by the (CIMEL) Sun photometer measurements. The CIMEL is an automatic Sun-sky scanning filter radiometer allowing the measurements of the direct solar irradiance at wavelengths; 340, 380, 440, 500, 670, 870, and 1020 nm. The CIMEL at Belsk is included in the NASA AERONET network and the data acquired is sent to the NASA Goddard Space Flight Center using a satellite data telemetry antenna. NASA provides preliminary processing of the real-time data containing the daily pattern of AOD at all operational wavelengths. Moreover, the sky radiance almucantar measurements are taken at spectral channels at 440, 670, 870, 1020 nm. For selected solar zenith angle, sky radiances are acquired in azimuth angles within the relative azimuth angle range (from the Sun) of 2°–180° [*Holben et al.*, 1998]. The

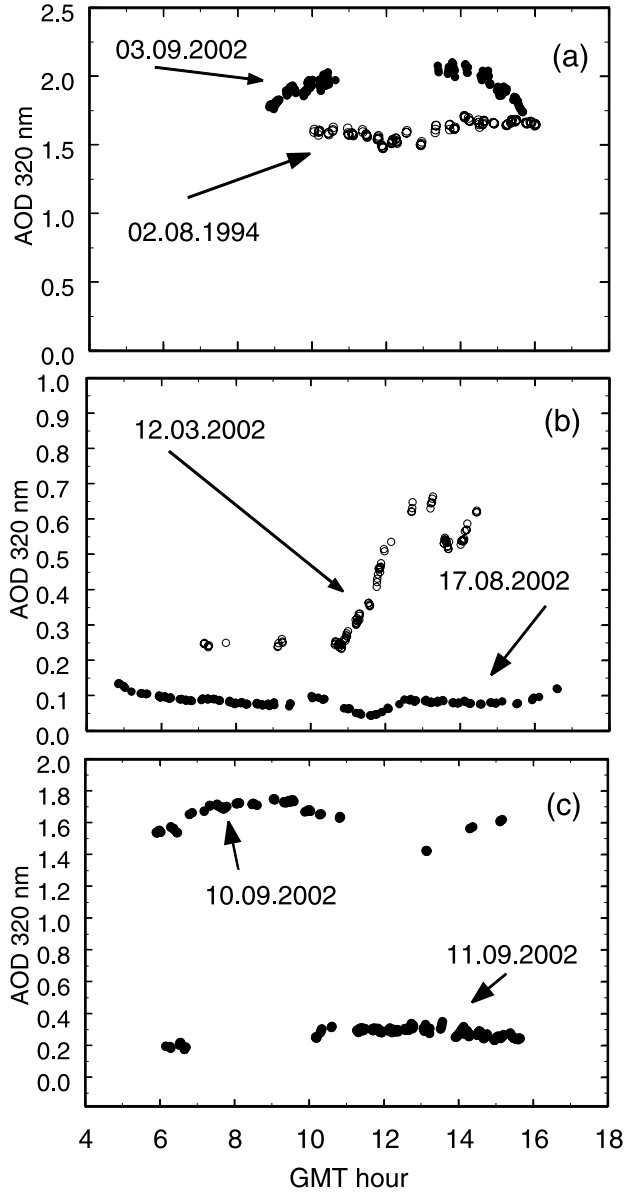

Figure 3. The daily pattern of the aerosol optical depth fluctuations at 319.8 nm for selected days.

AERONET inversion algorithm [*Dubovik and King*, 2000] provides the aerosol retrievals by fitting the entire measured field of Sun radiances and the angular distribution of sky radiances to a radiative transfer model that results in estimation of the aerosols size distribution, spectrally dependent complex refractive index, single scattering albedo, and asymmetry parameter.

3. Aerosols Variations in Various Timescales

[12] Time series of AOD daily means at 319.8 nm averaging results of all correct AOD measurements (the solar disc not obscured by clouds) taken at Belsk for the period July 1992 to December 2002 is shown in Figure 1. AOD during that period fluctuated within the range 0.04–1.90. The overall mean value was 0.35 ± 0.20 (1σ). A standard least squares fit to the data shown in Figure 1 gives statistically nonsignificant linear change (trend) in the AOD data for whole period of the observations. The solid curve in Figure 1 represents the long-term oscillations present in the data obtained by the application of the locally weighted regression (LOWESS) smoother to the daily AOD data. At each point in the data set a low-degree polynomial is fit to a subset of the data, with dependent variable values near the point whose smooth value is being estimated. The polynomial is fit using weighted least squares, giving more weight to points near the point whose response is being estimated and less weight to points further away [*Cleveland and Devlin*, 1988]. The level of smoothing is chosen to suppress the AOD oscillations with timescales shorter than 3–4 years. The pattern of long-period fluctuations shows the AOD decrease from ~0.5 to ~0.25 in the period 1992–1997, constant AOD level in 1997–2001, and enhanced aerosol loading in 2002. The negative AOD tendency in the 1992–1997 period can be partially related to decreasing aerosol loading in the stratosphere after the Pinatubo eruption (see dashed line in Figure 1 being the stratospheric AOD at 320 nm over 40°–50°N region from the combined satellite and ground-based observations [*Stevermer et al.*,

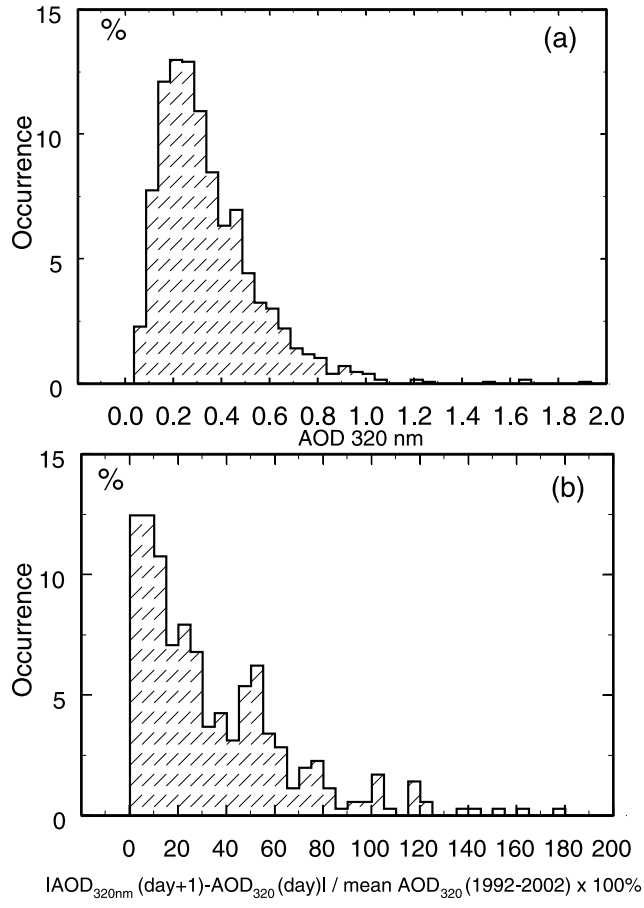

Figure 4. (a) Relative frequency of daily means of aerosol optical depth at 319.8 nm from the Brewer spectrophotometer measurements at Belsk for the period 1992–2002. (b) Relative frequency of 1-day changes of the aerosol optical depth at 319 nm, AOD(day + 1) – AOD(day), normalized to the overall mean of aerosol optical depth (0.35) in percent.

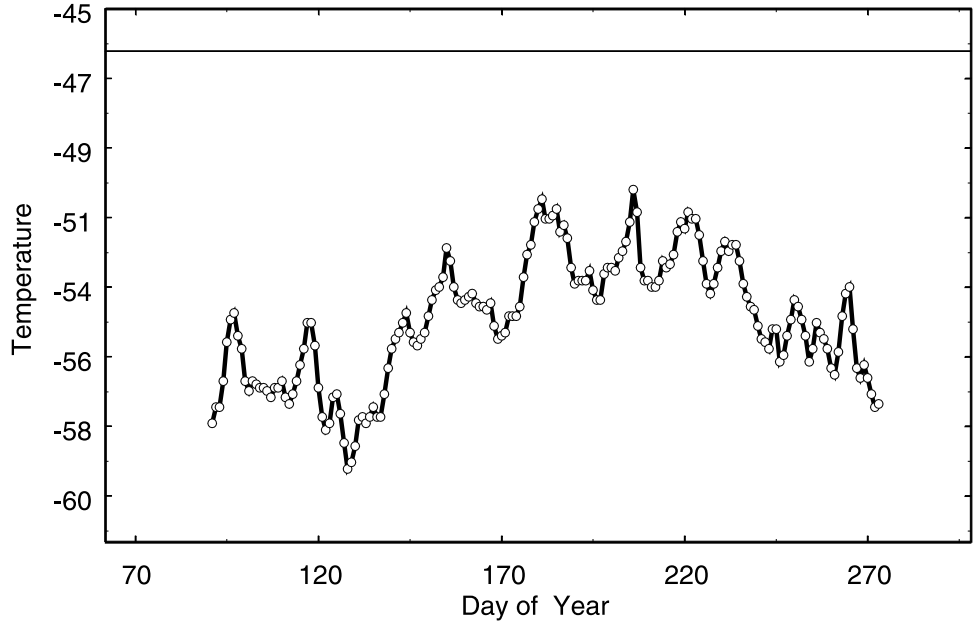

Figure 5. Time series of temperature at 50 hPa level over Belsk for the period April–October 2002 interpolated from the NCAR/NCEP Reanalysis data base. The straight line −46.3°C marks the standard stratospheric temperature used in the Brewer ozone retrieval.

2000], data prepared by the Surface Radiation Research Branch (SRRB) of NOAA's Air Resources Laboratory are presently available at address http://www.srrb.noaa.gov/research/aerdata.html). Moreover the changes in the Polish industry starting in the early 1990 (i.e., reduction of the coal burning and more care of the environment protection) can be also responsible for the atmosphere cleaning in the nineties [*Kopcewicz and Kopcewicz*, 2002]. Slightly larger mean AOD values appear in 2002. It is due to series of large AOD values during unusual summer with extremes in first half of September up to 1.9 there.

[13] The seasonal AOD pattern is shown in Figure 2. It appears that the late autumn and winter mean AODs are lower compared to those in summer but AOD measurements during late autumn/winter observations are not so frequent (on average there are only 7 days per month during the late autumn/winter and about 18 days per month in the summer months). Moreover, the winter observations are frequently carried out during the Arctic air masses advection with low aerosol loading. Extremely low AODs (<0.1) were observed at Belsk throughout the year independently on season while the extreme high AOD (>0.7) appeared in spring and summer. However, it seems possible to draw a straight line across the error bars that gives no seasonal variations. It may illustrate that the winter AOD data are not significantly lower than the spring/summer ones, i.e., large AOD variations within each month mask a seasonal pattern.

[14] The AOD at 319.8 nm variations throughout a day are shown in Figure 3. The daily pattern for extreme large AOD cases (2 August 1994 and 3 September 2002) is rather constant (Figure 3a). It seems impossible that so high AOD values appeared due to the cloud effects superimposed on the aerosol effects because clouds usually induce much larger variations of optical depth in timescales of minutes. The extreme large AOD values in summer 2002 were also noted over several East and Central European AERONET stations (posters of Torres et al., Synergic use of TOMS and AERONET observations for characterization of aerosol absorptions, and Chubarova and Riebou, The optical properties of atmosphere during natural fire experiment in Central Russia and their impact on UV irradiance, presented at EGS-AGU-EUG Joint Assembly, Nice, 6–11 April, 2003). At that time fires in the peat bog regions of east Poland and Byelorussia and Central Russia appeared (summer 2002 was extremely dry there) and the scales of fires and their effects on the air quality was so large that the public was alarmed (see CNN news at page http://www.cnn.com/2002/WORLD/europe/09/05/russia.smog). It should be noted that similar values of AOD were observed during biomass burning area over central Brazil [*Kirchhoff et al.*, 2001].

[15] The extreme low AOD case (17 August 2002) and the case with large daily variations of AOD (2 March 2002, see a smooth change of AOD throughout the day) are illustrated in Figure 3b. The day-to-day changes of AOD at 319.8 nm sometimes may be quite large (see change of AOD from ~1.7 on 10 September 2002 to 0.2 on 11 September 2002, Figure 3c). Thus, for the purpose of the UV Index forecasting it is of special importance to estimate how large are day-to-day changes in AOD since it has been established that the AOD impact on the UV daily doses in late spring and summer is comparable to that induced by the total ozone changes [*Krzyścin and Puchalski*, 1998]. Moreover, *Wenny et al.* [2001] discussed that assumption of constant (climatological mean) AOD might lead to large overestimation of the UV Index in summer, i.e., in the period when the knowledge of the UV irradiance is especially important.

[16] Frequency of the AOD appearance in selected intervals is presented in Figure 4a. Five percent of daily values

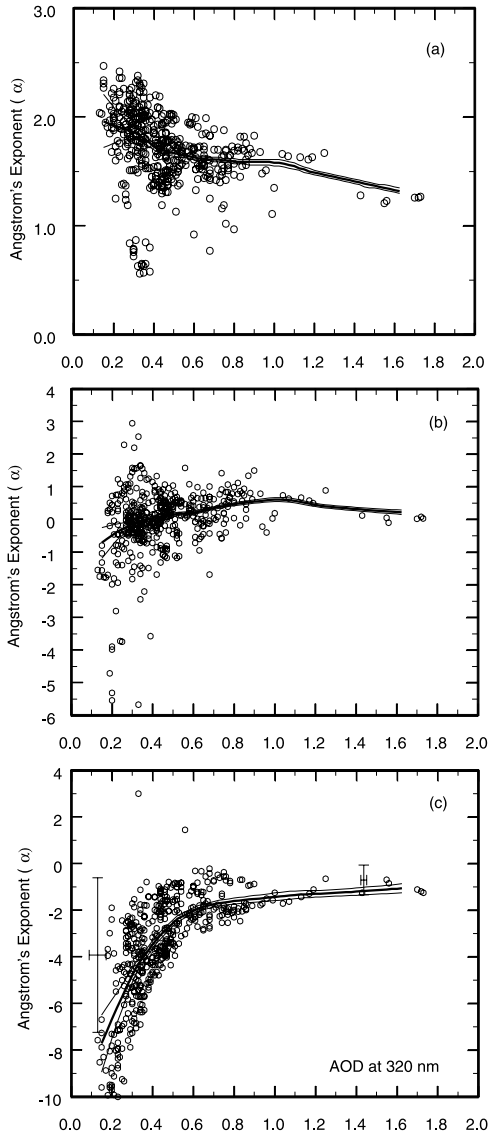

Figure 6. Ångström's exponent for various wavelength pairs: (a) 440–670 nm, (b) 310–340 nm, (c) 310–320 nm versus the aerosol optical depth at 319.8 nm from simultaneous measurements of aerosol optical depth by the Cimel Sun photometer and the Brewer spectrophotometer at Belsk for the period from April to October 2002. Thick solid curve represents the exponent dependence on the aerosol optical change derived from a smoother (LOWESS) applied to the data points. Thin solid curves represent the 99.9% confidence interval for the thick curve obtained by the bootstrap procedure discussed in the text.

were below (above) 0.11 (0.73). Figure 4b shows the histogram of the differences between the AOD daily means in two consecutive days in percent of the overall mean (0.35), 5% of such normalized 1-day changes of AOD are higher than 100%. Taking into account the radiation amplification factor due to AOD changes reported by *Krzyścin and Puchalski* [1998], about 0.1 in the warm period of the year (i.e., 10% decrease (increase) of AOD relative to its norm forces ∼1% increase (decrease) in the erythemal UV irradiace at the Earth's surface), we estimated that 5% of all analyzed 1-day changes of AOD would induce more than 10% change of the erythemal UV irradiance. The uncertainty level (random error) of the erythemally weighted UV irradiance measured by the broadband instruments (like Solar Light 501 series of the biometers) is estimated (by the producer) as about ±5%. Thus 1-day AOD change larger than 50% of the overall norm will induce the UV changes beyond the uncertainty range of the broadband instrument. Such changes appear in ∼30% of all analyzed cases. Thus, assuming the persistence of AOD, we can expect that in ∼70% of all cases the uncertainty in the clear-sky UV index forecast due to AOD variations not accounted by a UV index model is within the range of the UV dose rate measurement accuracy. In other words, in ∼30% of cases more precise forecast of AOD is needed.

4. Ångström Exponent in the UV Range

[17] The wavelength dependence of AOD in the visible range usually follows a power law with an exponent α called Ångström exponent [*Ångström*, 1929], $\tau(\lambda) \sim \lambda^{-\alpha}$, In the visible range α is a basic measure of the aerosol size distribution; $\alpha \sim 0$ corresponds to large dust particles, $\alpha \sim 2$ is associated to small smoke particles. *Woodman* [1974] summarized measurements carried under various meteorological conditions reported $\alpha = 1.3 \pm 0.6$. *Puchalski and Sobolewski* [2001] found $\alpha = 1.5 \pm 0.2$ analyzing spectral (390–667 nm) optical thickness at Belsk for the period 1993–1998. There were several studies [e.g., *Smirnow et al.*, 1995; *Wenny et al.*, 1998] on α changes according to synoptic air mass type and the aerosol origin (e.g., urban, rural, desert aerosols). *Kirchhoff et al.* [2001] show results of AOD spectral measurements by BS for its standard wavelengths (see their tables) but finding a formula describing AOD dependence on wavelength was beyond the scope of the paper. It can be inferred from their data that AOD frequently decreases for shorter wavelengths (i.e., α changes sign). *Wenny et al.* [2001], analyzing the results by a Yankee ultraviolet multifilter shadow-band radiometer, found that AOD in the UV-B range also decreased for shorter wavelengths (see their Figure 4). However, they discussed that it was probably the result of the AOD uncertainty resulting from strong UV absorption by total ozone not precisely resolved by the multifilter measurements.

[18] Calculation of the Ångström exponent in cases when considered wavelength is within the UV-B range requires precise estimation of the optical depth due to ozone (product of total ozone, ozone absorption coefficient, and air mass). The Belsk's BS has been regularly compared to a traveling standard and during calibrations only small ±1% errors were found. Moreover the instrument stability has been frequently checked with an internal standard lamp. Special attention should be paid to the temperature effect on the ozone optical depth. The standard Brewer ozone retrieval does not use actual stratospheric temperature, only one temperature value, −46.3°C, is assumed. Figure 5 shows temperature course over Belsk approximately at the level of ozone maximum (50 hPa in the warm period of the year) in the April–October 2002 period. The temperature data (interpolated to the station's location) are taken from the NCEP/NCAR Reanalysis data base (available at address: http://wesley.wwb.noaa.gov/ncep_data) comprising results of the ground-based (rawind-

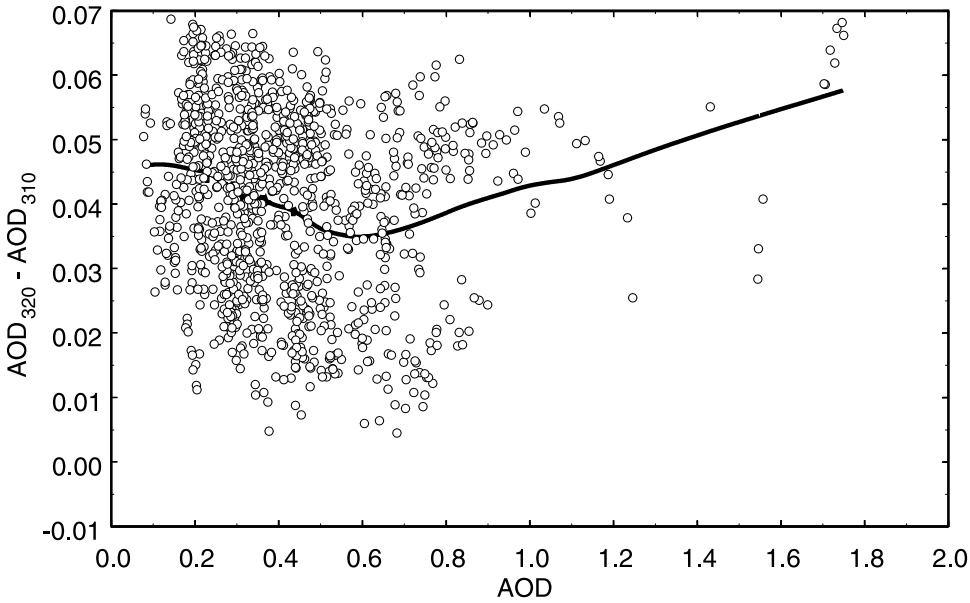

Figure 7. The difference between aerosol optical depth at 319.8 nm and 309.8 nm versus the aerosol optical depth at 319.8 nm for the Brewer spectrophotometer measurements in the period from April to October 2002.

soundings) and satellite observations of the atmosphere. It is seen that temperature at the level of ozone maximum is below the standard stratospheric temperature used by the Brewer algorithm. The corrected total ozone values, $Tot_{O3,\mathrm{corr}}$, accounting for the stratospheric temperature departures from the standard temperature can be expressed as [*Roozendael et al.*, 1998] $Tot_{O3,\mathrm{corr}} = Tot_{O3}/(1 + a(T + 46.3^{\circ}\mathrm{C}))$, where Tot_{O3} is output from the standard Brewer ozone retrieval software, T is actual stratospheric temperature approximately at the level of ozone maximum, and $\alpha = 0.0013/^{\circ}\mathrm{C}$. The corrected ozone values calculated with this formula and the temperature time series shown in Figure 5 are about 1–2% higher than those by standard Brewer retrieval. The ozone absorption cross sections are also calculated at actual stratospheric temperature. The combined temperature effect on the AOD retrieval (i.e., increase of total ozone and decrease of ozone absorption cross section relative to those calculated at standard temperature) leads to small change of AODs. For example, the temperature effect averaged over the April–October 2002 period yields the AOD changes <0.005 at the UV-B range relative to the values obtained at standard temperature.

[19] It should be noted that it is difficult to decide if Ångström formula fits the measured AOD at Belsk in the UV range because the analyzed UV wavelength span is rather tight (306.1, 309.8, 313.3, 316.6, 319.8 nm from BS and 340, 380 nm from the CIMEL) and the expected AOD changes over the UV range are not large precluding precise determination of the AOD spectral shape. However we calculate the Ångström exponent (AE) for selected UV wavelength pairs to estimate a direction of the AOD change in the UV range (increase or decrease of AOD with wavelengths) rather than to discuss if power law still fits the AOD dependence over UV wavelengths.

[20] In Figure 6 we show AE versus AOD at 319.8 nm for all simultaneous measurements (~1000 data points) by CIMEL and BS in the period April–October 2002 for the following pairs: 440–670 nm ($\alpha_{440-670}$, only the CIMEL data, Figure 6a), 309.8–340 nm ($\alpha_{310-340}$, mixed BS and CIMEL data, Figure 6b), and 309.8–319.8 nm ($\alpha_{310-320}$, only BS data, Figure 6c). As it was expected $\alpha_{440-670}$ is always positive and decreases only slightly with AOD for the visible range. The overall mean $\alpha_{440-670} = 1.71 \pm 0.35$ (1σ), which is only slightly larger than the value reported by *Puchalski and Sobolewski* [2001]. For the 340–380 nm pair (results for this pair are not shown in Figure 6) the change of AOD with wavelength shows less slope relative to that calculated for the visible range, $\alpha_{340-380} = 1.06 \pm 0.46$ (1σ). AE seems to decrease further if shorter wavelength pair is selected (see Figures 6b and 6c). An apparent dependence of $\alpha_{310-340}$ and $\alpha_{310-320}$ on AOD (increase from large negative value to slightly positive (Figure 6b) or negative values (Figure 6c)) can be inferred from the smoothed pattern (by LOWESS) of the AE variations.

[21] Taking into account the AOD uncertainty, the errors bars are drawn in Figure 6c for two points (small and large AOD at 319.8 nm) to illustrate possible range of the random fluctuations of AE. It is seen that the AE uncertainties are quite large especially for low aerosol loading. To support the negative AE values in the UV range we estimate 99.9% confidence interval for the LOWESS curves present in Figure 6 using the bootstrap technique. The following steps are repeated 10000 times; random normal noise (with zero mean and standard deviation equal to the AOD uncertainty) is added to each measured AOD, hypothetical AE are calculated and smoothed by LOWESS, the smoothed AE values are stored for selected AOD values at 319.8 nm (0.1, 0.15, . . ., 1.65). Thus, finally, we have 10000 hypothetical AE values for selected AOD at 319.8 nm. By drawing AE values representing 0,05% and 99.95% point in the ordered (in ascending way) AE set we estimate 99.9% confidence interval for the smoothed AE values (thin solid curves in Figure 6). As it is seen in Figure 6, the possible variations of

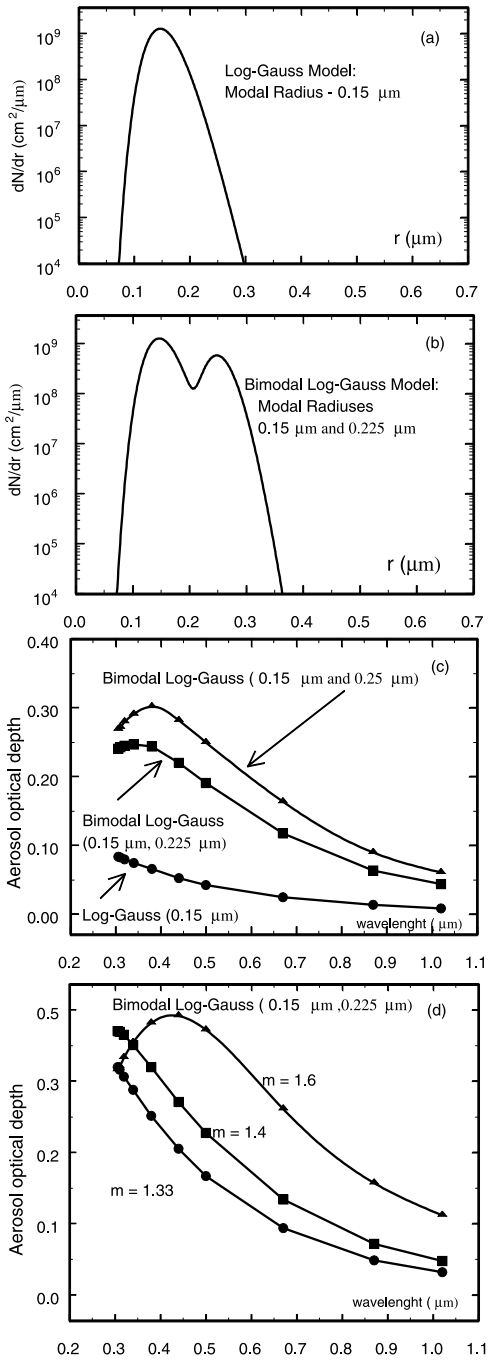

Figure 8. (a) Aerosol size distribution as given by single log-Gauss distribution with modal radius 0.15 μm. (b) Aerosol size distribution as given by bimodal log-Gauss distribution with modal radius 0.15 μm and 0.225 μm. (c) Aerosol optical depth dependence on wavelength for various aerosol size distribution (single log-Gauss and various bimodal log-Gauss distributions) for the refractive index equal to 1.5. (d) Aerosol optical depth dependence on wavelength for bimodal log-Gauss distribution shown in Figure 8b for various refractive indices.

the smoothed AE pattern are rather limited even for small AOD at 319.8 nm. It should be noted that 99.9% confidence interval is below line AE = 0 (Figure 6c) suggesting negative value of AE over whole AOD range and an increase of AE with AOD (opposite to AE behavior over visible wavelength). The large negative AE values do not mean the large differences between AOD at 320 and 310 nm. AODs at 310 nm are only few hundredths lower than those at 320 nm (Figure 7).

[22] We would like to find a theoretical evidence for different (even negative) α values in the UV range compared to those in the visible range. We calculate AOD using the following formula,

$$\tau(\lambda) = \int \pi r^2 Q_{ext}(\lambda, r, m) n(r) dr \tag{3}$$

where: Q_{ext} (λ, r, m) is the extinction efficiency factor depending on wavelength (derived from the Mie's theory), particle radii r, and refraction index m, n is aerosol volume size distribution. Figures 8a and 8b show examples of the aerosol size distribution, i.e., single log-Gauss and bimodal log-Gauss distributions. Bimodal log-Gauss distribution is defined as follow;

$$\frac{dn}{dr} = N_1 f(r_1, r_{10}, R_1) + N_2 f(r_2, 2_{20}, R_2)$$
$$f(r, r_0, R) = 0.434 \sqrt{\frac{R}{\pi}} r \exp\left[-R\left(\log\frac{r}{r_0}\right)^2\right] \tag{4}$$

where N_i is the total particle number for fraction ith in the column of atmosphere of 1 cm^2 cross section, r_{io} is the modal radius, and R_i is a parameter describing the dispersion of the particles. Single log-Gauss is a simplified version of (4) with $N_2 = 0$. *Puchalski and Sobolewski* [2001] discussed that distribution (4) could represent the aerosol size distribution inferred from the spectral AOD measurements at Belsk by four-channel Linke's Sun radiometer in the 1993–1998 period.

[23] The AOD dependence on wavelength for single log-Gauss (Figure 8a) and various bimodal log-Gauss distribution (Figure 8b) are shown in Figure 8c. Symbols on Figure 8c represent the AOD values at 310, 320, 340, 380, 440, 500, 660, 870, and 1020 nm. i.e., for the BS and CIMEL characteristic wavelengths. It is seen that some aerosol compositions yield the AOD decrease for shorter wavelengths. The AOD patterns shown in Figure 8c have been calculated assuming $m = 1.5$. We also obtain the AOD pattern keeping constant bimodal log-Gauss aerosol distribution as shown in Figure 8b but changing m values. It is found (Figure 8d) that small m values (1.33, 1.40) provides the AOD increase for shorter wavelengths for all considered wavelengths, whereas larger m yields the AOD decrease over UV range ($m = 1.5$ in Figure 8c) and even in both UV and visible range ($m = 1.6$ in Figure 8d). Thus both combination of the aerosol composition and refractive properties of aerosol could yield negative AE values in the UV range. It looks that smaller values or even negative values of AE in the UV range found by the statistical analysis are not a statistical or instrumental error. They have a physical foundation resulting from the Mie scattering for specific combination of wavelength, particle radii, and refractive index.

5. Summary

[24] With a Brewer spectrophotometer an estimation of AOD can be derived based on standard direct Sun observations routinely used in a calculation of total ozone. Thus

existing relatively long-term series of direct Sun measurements by Brewer instruments may be used for retrieval of AOD. Here AOD at the UV-B and short UV-A wavelengths has been constructed for the period 1992–2002 using the direct Sun radiances measured at Belsk. The long-term variations appear to be trendless with only small year-to-year variations not affecting the UV level at the Earth's surface.

[25] Because of difficulties to measure AOD at UV region and predict changes in the aerosol loading of the atmosphere a constant AOD value (climatological mean) is usually taken to calculate the maximum value (clear-sky) of the next day UV Index [e.g., *De Backer et al.*, 2001]. The statistical analysis of the 1-day change of AOD at the UV range shows that in 30% of cases the scale of the aerosol change is important for the next day UV Index forecast, i.e., inducing a change in the UV index larger than ±5%.

[26] Analyzing dependence of AOD on wavelength we combine CIMEL Sun photometer and the Brewer spectrophotometer optical depth data. We calculate the Ångström's exponent for the pairs of wavelengths in the visible, UV-A, and UV-A/UV-B range to examine if the values taken at visible range can be extrapolated to shorter wavelengths. It is found that Ångström's exponent decreases for the pair with shorter wavelengths and it becomes possible that in the UV-B/UV-A range the exponent is negative yielding an increase of aerosol optical depth with wavelength. Moreover, in the visible range it seems that larger exponent values are associated with low aerosol days. The opposite is found for the exponent dependence on AOD in the UV range. More negative exponent appears for low aerosols days yielding the steeper wavelength dependence (increase with wavelength) than for high aerosol days. The Mie code simulations corroborate the hypothesis of possible negative value for the Ångström's exponent for the UV-B/UV-A pair of wavelengths.

[27] **Acknowledgments.** The study has been supported by the Commission of the European Communities through EDUCE project contract EVK2-CT-1999-00028 and by the State Inspectorate for Environmental Protection, Poland, under contract 359/2001/Wn50/MN-PO-BD/D.

References

Ångström, A., On the atmospheric transmission of Sun radiation and on dust in the air, *Geogr. Ann.*, *11*, 156–166, 1929.

De Backer, H., et al., Comparison of measured and modelled UV indices for the assessment of health risks, *Meteorol. Appl.*, *8*, 267–277, 2001.

Bais, A. F., Absolute spectral measurements of the direct solar ultraviolet irradiance using a Brewer spectrophotometer, *Appl. Opt.*, *36*, 5199–5204, 1997.

Bass, A. M., and R. J. Paur, The ultraviolet cross-sections of ozone: I. The measurements in Atmospheric ozone, in *Atmospheric Ozone, Proceedings of the Quadrennial Ozone Symposium Held in Halkidiki, Greece, 3–7 September 1984*, edited by C. S. Zerefos and A. Ghazi, pp. 606–610, D. Reidel, Norwell, Mass., 1985.

Bernhard, G., and G. Seckmeyer, The uncertainty of measurements of spectral solar UV irradiance, *J. Geophys. Res.*, *104*, 14,321–14,345, 1999.

Brewer, A. W., A replacement for the Dobson spectrophotometer?, *Pure Appl. Geophys.*, *106–108*, 919–927, 1973.

Bucholtz, A., Rayleigh-scattering calculations for terrestrial atmosphere, *Appl. Opt.*, *34*, 2765–2773, 1995.

Cleveland, W. S., and S. J. Devlin, Locally weighted regression: An approach to regression analysis by local fitting, *J. Am. Stat. Assoc.*, *83*, 596–610, 1988.

Dubovik, O., and M. D. King, A flexible inversion algorithm for retrieval of aerosol optical properties from Sun and sky radiance measurements, *J. Geophys. Res.*, *105*, 20,673–20,696, 2000.

Holben, B. N., et al., AERONET—A federated instrument network and data archive for aerosol characterization, *Remote Sens. Environ.*, *66*, 1–16, 1998.

Holben, B. N., et al., An emerging ground-based aerosol climatology: Aerosol optical depth from AERONET, *J. Geophys. Res.*, *106*, 12,067–12,097, 2001.

International Standards Organization (ISO), *Guide to the Expression of Uncertainty in Measurement*, Geneva, Switzerland, 1993.

Jarosławski, J., and J. W. Krzyścin, Aerosol optical depth in the UV range derived from direct Sun observations performed by the Brewer spectrophotometer, in *Atmospheric Ozone (Proceedings of the Quadrennial Ozone Symposium)*, Hokkaido Univ. Press, Sapporo, Japan, 2000.

Kopcewicz, B., and M. Kopcewicz, Trends in atmospheric iron measured by Mössbauer spectroscopy, *Hyperfine Interactions (c)*, Vol. *5*, 427–430, 2002.

Kirchhoff, V. W. J. H., A. A. Silva, C. A. Costa, N. Paes Leme, H. G. Pavão, and F. Zaratti, UV-B optical thickness observations of the atmosphere, *J. Geophys. Res.*, *106*, 2963–2973, 2001.

Krzyścin, J. W., and S. Puchalski, Aerosol impact on the surface UV radiation from the ground-based measurements taken at Belsk, Poland, 1980–1996, *J. Geophys. Res.*, *103*, 16,175–16,181, 1998.

Krzyścin, J. W., J. Jarosławski, and P. Sobolewski, On an improvement of UV index forecast: UV index diagnosis and forecast for Belsk, Poland, in spring/summer 1999, *J. Atmos. Sol. Terr. Phys.*, *63*, 1593–1600, 2001.

Liu, S. C., S. A. McKeen, and S. Madronich, Effects of anthropogenic aerosols on biologically active ultraviolet radiation, *Geophys. Res. Lett.*, *18*, 2265–2268, 1991.

Marenco, F., V. Santacesaria, A. F. Bais, D. Balis, A. di Sarra, A. Papayannis, and C. S. Zerefos, Optical properties of tropospheric aerosols determined by lidar and spectrophotometric measurements (PAUR campaign), *Appl. Opt.*, *36*, 6875–6886, 1997.

Marenco, F., A. di Sarra, and J. De Luisi, Methodology for determining aerosol optical depth from Brewer 300–320 nm ozone measurements, *Appl. Opt.*, *41*, 1805–1814, 2002.

Meleti, C., and F. Cappellani, Measurements of aerosol optical depth at Ispra: Analysis of the correlation with UV-B, UV-A, and total solar irradiance, *J. Geophys. Res.*, *105*, 4971–4978, 2000.

Puchalski, S. P., and P. S. Sobolewski, Spectral optical thickness and aerosol size distribution of air columns at Belsk in 1993–1998, *Acta Geophys. Polonica*, *49*, 261–270, 2001.

Roozendael, M., et al., Validation of ground-based visible measurements of total ozone by comparison with Dobson and Brewer spectrophotometer, *J. Atmos. Chem.*, *29*, 55–83, 1998.

Smirnow, A., Y. Villevalde, N. T. O'Neill, A. Royer, and A. Tarussov, Aerosol optical depth over oceans: Analysis in terms of synoptic air mass types, *J. Geophys. Res.*, *100*, 16,639–16,650, 1995.

Stevermer, A. J., I. Petropavlovskikh, J. M. Rosen, and J. J. DeLuisi, Development of a global stratospheric aerosol climatology: Optical properties and applications for UV, *J. Geophys. Res.*, *105*, 22,763–22,776, 2000.

Wenny, B. N., J. S. Schafer, J. J. DeLuisi, V. K. Saxena, W. F. Barnard, I. V. Petropavloskikh, and A. J. Vergamini, A study of regional aerosol radiative properties and effects on ultraviolet-B radiation, *J. Geophys. Res.*, *103*, 17,083–17,097, 1998.

Wenny, B. N., V. K. Saxena, and J. E. Frederick, Aerosol optical depth measurements and their impact on surface levels of ultraviolet-B radiation, *J. Geophys. Res.*, *106*, 17,311–17,319, 2001.

Woodman, D. F., Limitation in using atmospheric models for laser transmission estimates, *Appl. Opt.*, *13*, 2193–2195, 1974.

Zerefos, C., Factors influencing the transmission of the solar ultraviolet irradiance through the Earth's atmosphere, in *Solar Ultraviolet Radiation, Modelling Mesurements and Effects*, *NATO ASI Ser., Ser. I*, vol. 52, edited by C. S. Zerefos and A. F. Bais, pp. 133–141, Springer-Verlag, New York, 1997.

Zerefos, C. S., C. Melleti, A. F. Bais, and A. Lambros, The recent UVB variability over southeastern Europe, *Photochem. Photobiol.*, *20*, 15–19, 1995.

J. Jarosławski, J. W. Krzyścin, S. Puchalski, and P. Sobolewski, Institute of Geophysics, Polish Academy of Sciences, 01-452 Warsaw, Poland. (jkrzys@igf.edu.pl)